Talanta 175 (2017) 318–324

Contents lists available at ScienceDirect

Talanta

journal homepage: www.elsevier.com/locate/talanta

Radiometric evaluation of diglycolamide resins for the chromatographic separation of actinium from fission product lanthanides

Valery Radchenko[a,b], Tara Mastren[a], Catherine A.L. Meyer[a], Alexander S. Ivanov[c], Vyacheslav S. Bryantsev[c], Roy Copping[d], David Denton[d], Jonathan W. Engle[a,e], Justin R. Griswold[d], Karen Murphy[d], Justin J. Wilson[a,f], Allison Owens[d], Lance Wyant[c], Eva R. Birnbaum[a], Jonathan Fitzsimmons[g], Dmitri Medvedev[g], Cathy S. Cutler[g], Leonard F. Mausner[g], Meiring F. Nortier[a], Kevin D. John[a], Saed Mirzadeh[d], Michael E. Fassbender[a,*]

[a] *Chemistry Division, Los Alamos National Laboratory, P.O. Box 1663, Los Alamos, NM 87545, USA*
[b] *Life Science Division, TRIUMF, 4004 Wesbrook Mall, Vancouver, BC V6T 2A3, Canada*
[c] *Chemical Sciences Division, Oak Ridge National Laboratory, Oak Ridge, TN 37831, USA*
[d] *Nuclear Security and Isotope Technology Division, Oak Ridge National Laboratory, Oak Ridge, TN 37831, USA*
[e] *Department of Medical Physics, University of Wisconsin, Madison, WI 53705, USA*
[f] *Department of Chemistry & Chemical Biology, Cornell University, Ithaca, NY 14853, USA*
[g] *Collider-Accelerator Department, Brookhaven National Laboratory, Bldg 801, Upton, NY 11973, USA*

ARTICLE INFO

Keywords:
^{225}Ac
Lanthanide separation
Extraction chromatography
Diglycolamide resins
Distribution coefficients
Gibbs sorption energy

ABSTRACT

Actinium-225 is a potential Targeted Alpha Therapy (TAT) isotope. It can be generated with high energy (≥ 100 MeV) proton irradiation of thorium targets. The main challenge in the chemical recovery of ^{225}Ac lies in the separation from thorium and many fission by-products most importantly radiolanthanides. We recently developed a separation strategy based on a combination of cation exchange and extraction chromatography to isolate and purify ^{225}Ac. In this study, actinium and lanthanide equilibrium distribution coefficients and column elution behavior for both TODGA (N,N,N′,N′-tetra-*n*-octyldiglycolamide) and TEHDGA (N,N,N′,N′-tetrakis-2-ethylhexyldiglycolamide) were determined. Density functional theory (DFT) calculations were performed and were in agreement with experimental observations providing the foundation for understanding of the selectivity for Ac and lanthanides on different DGA (diglycolamide) based resins. The results of Gibbs energy (ΔG_{aq}) calculations confirm significantly higher selectivity of DGA based resins for Ln^{III} over Ac^{III} in the presence of nitrate. DFT calculations and experimental results reveal that Ac chemistry cannot be predicted from lanthanide behavior under comparable circumstances.

1. Introduction

Targeted alpha therapy (TAT), is a method utilized to treat cancer and other diseases through the attachment of appropriately selected α-emitting radionuclides to targeting biomolecules (i.e. steroids, peptides, antibodies, antibody fragments), usually through conjugation of an appropriate chelate that is specific to the radionuclide of interest [1–3]. The U.S. Food and Drug Administration (FDA) has recently approved the use of $^{223}RaCl_2$ for pain relief from bone metastases, and early results obtained from clinical and pre-clinical studies on other alpha radionuclides [4] are promising. These developments indicate that clinical applications of TAT in the near future are becoming increasingly plausible. The primary limitation is the availability of α-emitting radionuclides. Irradiations of target nuclei with high atomic numbers (> 82) are required to form most candidate α-emitters. Therefore, high costs are encountered when producing and processing these isotopes, and appropriate technologies must be developed to realize their potential. Actinium-225 ($t_{1/2}$ = 9.92 days) is one of the most promising TAT radionuclides and has shown high potential [5]. Its half-life matches the biological half-lives of intact antibodies; it also yields the benefit of decaying into multiple α-emitting daughters thus enhancing the therapeutic effect. Currently, the main source of ^{225}Ac is from the radioactive decay of ^{229}Th ($t_{1/2}$ 7920 a). This limits the annual available quantity of ^{225}Ac to ≤ 63 GBq/year (1.7 Ci/year) worldwide [5].

* Corresponding author.
E-mail address: mifa@lanl.gov (M.E. Fassbender).

http://dx.doi.org/10.1016/j.talanta.2017.07.057
Received 23 June 2017; Received in revised form 18 July 2017; Accepted 19 July 2017
Available online 20 July 2017

In an effort to increase the availability of ^{225}Ac the US Department of Energy has initiated a multi-national lab project (including Los Alamos, Brookhaven and Oak Ridge National Laboratories) in support of the production of ^{225}Ac via irradiation of thorium metal targets. Previously acquired data demonstrated that a 10- day irradiation with a proton beam intensity of 250 μA and beam energy range of 93 → 72 MeV (5 g·cm^{-2} thickness Th metal), would result in the formation of 73.3 GBq (1.98 Ci) of ^{225}Ac [6]. One of the many challenges associated with this method is the requirement of efficient chemical separation to provide a high purity product for radiopharmaceutical applications.

To isolate quasi massless quantities of ^{225}Ac from the bulk thorium target and co-produced fission products, a previously developed separation method [7] was followed initially, and an alternative separation has recently been developed and tested on an analytical scale [8]. A vital component in the separation strategy for the purification of Ac is the removal of fission generated lanthanide isotopes, which are chemically very similar to actinium. This requires careful control of elution conditions. A method for actinium (Ac)/lanthanide (Ln) separation using a DGA (diglycolamide) based extraction chromatographic system was developed and demonstrated on the analytical scale [8]. This preliminary investigation of Ac/Ln separation indicates that separation of Ac from Ln can be achieved in HNO_3 media while a subsequent separation of individual members of Ln may be efficiently performed in HCl media. Therefore, further investigation of the separation parameters governing Ac/Ln separation on DGA based extraction chromatography systems was desired.

In this study, we present K_d substantiated parameters for the extraction chromatographic separation of Ac from radio-Ln and for the separation of radio-Ln from each other. Distribution coefficients for Ac and Ln (III) in HNO_3 and HCl media have been reported before [9–16], but not within the acid concentration ranges where a difference in sorption behavior between Ac and lanthanides becomes analytically relevant. Especially with respect to HNO_3, literature Ac sorption data does not accurately describe the higher concentration range (> 4 M), which we deem crucial to corroborate the trend of decreasing Ac sorption at the simultaneous increase of Ln(III) retention as observable at lower matrix concentrations. The situation is similar for Ln(III) sorption in HCl media; published data [9–16] are largely limited to lower acid concentrations and fail to frame an insightful picture for concentrations > 6 M. A better understanding in this range could lead to the development of new f-element analytical applications.

As Ce was included in a previous study [8], two different Ln, one medium mass (Eu) and one heavier mass (Lu) element, were used to investigate Ln sorption behavior on DGA based extraction resins in this work. Both normal DGA (N,N,N′,N′-tetra-*n*-octyldiglycolamide; abbreviated TODGA herein after) and branched DGA (N,N,N′,N′-tetrakis-2-ethylhexyl-diglycolamide; abbreviated TEHDGA) resins were studied. Actinium/Ln separation factors in HNO_3 media can be deduced from conclusive literature K_d values [15,16]. Consequently, Ln K_d values in HNO_3 media were not measured in our study. Actinium K_d values in HNO_3 media in both TODGA and TEHDGA resins, on the other hand, were measured due to a lack of data consistency. Furthermore, density functional theory (DFT) modeling was carried out in order to shed light on the separation mechanism involving DGA ligands in HNO_3 media. Additional separation experiments with proton irradiated thorium targets were conducted to evaluate the suitability of TEHDGA resin for ^{225}Ac recovery purposes.

2. Experimental

2.1. Chemicals

All chemicals were used without further purification. Nitric acid (HNO_3) and hydrochloric acid (HCl), both Optima grade, were purchased from Fisher Scientific (Pittsburgh, PA, USA). Citric acid (99.9%) was obtained from Sigma Aldrich (St Louis, MO, USA), and deionized water (≥ 18 MΩ cm) was prepared on site with a Millipore water purification system. Cation exchange resin (AG 50WX8, 200–400 mesh) and anion exchange resin (AG 1-X8 200–400 mesh) were obtained from Bio-Rad (Hercules, CA, USA). Normal DGA resin (TODGA) and branched DGA resin (TEHDGA) were purchased from Eichrom Inc, (Lisle, IL, USA). Biorad Econo-columns (4.0 cm × 0.8 cm, Biorad Hercules, CA, USA) were used for all chromatography work throughout this study except for the remote-controlled target process, where a Bio-Rad glass column (15 cm × 0.5 cm) was used.

2.2. Gamma-ray spectrometry

Gamma-ray spectrometry for the distribution coefficients and dynamic column separation studies was conducted using an EG & G Ortec Model GMX-35200-S HPGe detector system in combination with a Canberra Model 35-Plus multichannel analyzer. Detector diameter was 50.0 mm; detector length 53.5 mm; Be window thickness 0.5 mm; outer dead-layer thickness 0.3 μm. Detector response function determination and evaluation were performed using standards of radionuclide mixtures containing ^{241}Am, ^{109}Cd, ^{57}Co, ^{139}Ce, ^{203}Hg, ^{113}Sn, ^{137}Cs, ^{88}Y, ^{60}Co, traceable to the National Institute of Standards and Technology (NIST) and supplied by Eckert & Ziegler, Atlanta, GA, USA. The detector was a p-type Al-windowed HPGe detector with a measured FWHM at 1333 keV of approximately 2.2 keV and a relative efficiency of about 10%. Relative total source activity uncertainties ranged from 2.6% to 3.3%. Counting dead time was kept below 10%. The γ-ray spectrometry for the irradiated target experiment is described in the Supporting information.

2.3. Radionuclides

Actinium-225 was obtained from a ^{229}Th generator (5.8 MBq, 156.7 μCi) available at LANL according to a procedure as described earlier [8]. In brief, ^{229}Th in decay equilibrium with ^{225}Ac dissolved in 8 M HNO_3 (5 mL) was loaded on a preconditioned anion exchange column (2 mL). At this condition, ^{229}Th was quantitatively retained on the column while ^{225}Ra and ^{225}Ac eluted without sorption. This mixture was utilized for the dynamic column experiments to demonstrate Ra/Ac separation capability along with additional ^{223}Ra tracer that was obtained as a decay product from an ^{227}Ac generator (40 MBq, 1.1 mCi). For the K_d studies, the ^{225}Ra/^{225}Ac eluent from the ^{229}Th generator was further purified to remove ^{225}Ra using TEHDGA resin: the fraction (1 mL) eluting from the anion exchange column was diluted to 4 M HNO_3, and was contacted with TEHDGA resin. Radium-225 eluted without sorption while ^{225}Ac was retained on the resin. The resin column was washed with additional 4 M HNO_3 to remove residual ^{225}Ra, and ^{225}Ac was stripped from the column with low molar (0.1 M) nitric acid. A HNO_3 solution of ^{155}Eu ($t_{1/2}$ = 4.76 a) was purchased from Eckert and Ziegler (Valencia, CA, USA), and ^{173}Lu ($t_{1/2}$ 1.37 a) was available from LANL's radionuclide inventory in an HCl matrix.

2.4. Proton irradiations

Samples for the *proof-of-principle experiment* and the *TEHDGA implementation study* were obtained from Th metal targets irradiated at the Isotope Production Facility (IPF), Los Alamos National Laboratory and the Brookhaven Linac Isotope Producer (BLIP). Targets were irradiated with 90 and 190 MeV incident energy protons as previously described [17].

2.5. Distribution coefficients

Equilibrium distribution coefficients (K_d values) were determined in triplicate by the batch method in nitric (HNO_3) and hydrochloric (HCl) acid media. For each determination, approximately 50 mg of

Table 1
Media concentrations and sample activities used in the distribution coefficient study.

HCl media			
Concentrations [M]	Activity [kBq] ^{225}Ac	^{155}Eu	^{173}Lu
0.1; 2; 4; 6; 8; 10; 11.5	5.93 ± 0.41	1.75 ± 0.08	2.88 ± 0.17
HNO_3 media			
0.1; 2; 4; 6; 8; 10; 12	2.97 ± 0.16		

resin (TODGA and TEHDGA, dry) was placed in a 2 mL sample tube, to which 1.00 ± 0.06 mL of solutions of varying acid matrix concentrations and 1–10 μL of the respective radionuclide stock were added (Table 1).

Mixtures were stirred vigorously and allowed to equilibrate for 24 h at room temperature. The mixtures were filtered and the filtrate added to pre-weighed 2 mL sample tubes. Solutions of ^{225}Ac were stored for 24 h to allow ^{225}Ac to reach equilibrium with its daughter radionuclides prior to γ-ray spectrometric analysis. The activities in the solid (resin) phases were determined by subtraction of activity in the solution from total activity in the sample. Distribution coefficients were calculated using Eq. (1), where $A_{50\ mg(res.)}$ is the activity in 50 mg of the resin and $A_{50\ \mu L(sol.)}$ is the activity in 50 ± 5 μL of solution.

$$K_D = \frac{C^{eq.}_{phase1}}{C^{eq.}_{phase2}} = \frac{A_{1g\,(res.)}}{A_{1mL\,(sol.)}} = \frac{A_{50mg\,(res.)}}{A_{50\mu L\,(sol.)}} \quad (1)$$

Uncertainties in equilibrium distribution coefficient values were calculated as the sum of the random activity measurement uncertainties in quadrature. Trend lines were software generated (MS Excel 2010).

2.6. Dynamic column separation experiments

Based on measured equilibrium distribution coefficients, dynamic column separation conditions were established. Bio-Rad plastic columns were filled with 1 mL of TODGA and TEHDGA, respectively. In a typical experiment, the column was preconditioned with water (2 mL) and 6 M HNO_3 (5 mL). A solution spiked with ^{225}Ra/Ac (6.0 kBq), ^{150}Eu (1.8 kBq) and ^{173}Lu (2.9 kBq) in 6 M HNO_3 was loaded onto the column (5 mL). The column was then washed with 4 M HNO_3 (5 mL). Subsequently, the column was eluted with 10 M HNO_3 (volumes of 15, 5 and 15 mL respectively) and 0.1 M HNO_3 (10 mL). Finally, the column was contacted with 0.1 M HCl (3 × 5 mL and 1 × 25 mL).

2.7. Irradiated target experiments and Ac separation in GBq quantities

A brief overview of the irradiated target dissolution and processing under master-slave manipulator control in a hot cell at ORNL is detailed elsewhere [17]. In short, the recovery process comprises two column-chromatographic steps. During the first step, Ac, Ln and Ra are retained on a cation exchanger column in a citrate matrix while bulk Th elutes. Actinium, Ra and La are then eluted from the cation column and further separated on a DGA column. Two studies were conducted in this work, a *proof of principle* study and a full scale TEHDGA implementation study. For the *proof-of-principle study*, two separate experiments with increasing radioactivity were performed: (1) First, an aliquot of an irradiated thorium target, representing ~ 2 × $10^{-3\%}$ of target solution at ~ 10 days post end of bombardment (EOB) was utilized. The DGA loading solution contained kBq (sub microcurie) quantities of radioisotopes of Ba, Ra, Ac, Ce and La serving as radiotracers in 6 M HNO_3 (20 mL). This solution (20 mL volume) was loaded on a TEHDGA resin column (1 mL volume resin bed), preconditioned with 6 M HNO_3 (5 mL). The load solution was collected and analyzed. The column was washed with an additional 10 mL of 6 M HNO_3 (5 mL each). Afterwards, the column was contacted with 10 M HNO_3 to elute the actinium (portions of 25 mL, 10 mL, 5 mL, and 10 mL). Finally, Ln elements were eluted with 0.1 M HNO_3 (5 mL). The eluted column was analyzed for residual activity.

(2) To confirm the elution profile on TEHDGA, an additional experiment was conducted utilizing a larger portion of the produced activity containing ^{225}Ac (118 MBq), ^{141}Ce (581 MBq), ^{147}Nd (110 MBq), ^{148}Pm (89 MBq) and ^{140}Ba (15 MBq) in 6 M nitric acid. This solution was loaded on TEHDGA (0.5 mL bed volume, BV) resin that was pre-conditioned with 6 M HNO_3. The column was washed with 6 M HNO_3 (8 BV) and then the Ac eluted (95%) with 10 M HNO_3 and collected in 4 BV fractions up to 25 mL. The column was then washed with 20 mL of 0.1 M HNO_3 and collected in 4 BV fractions. For the full scale implementation of TEHDGA for Ac/Ln separation, a proton irradiated thorium target was dissolved in HCl/HF media [17] in a hot cell under master-slave manipulator control at ORNL. TEHDGA resin (0.5 mL) was placed in a Bio-Rad glass column and preconditioned with 6 M HNO_3 (2 mL). The column was transferred to the hot cell. The post-cation column Ac/Ln fraction containing several GBq of ^{225}Ac with small quantities of long-lived isotope ^{227}Ac ($t_{1/2}$ 21.8 a) and similar activity levels of ^{141,144}Ce, ^{140}La as well as other Ra and Ba isotopes was loaded in 6 M HNO_3. The column was then washed with 4 M HNO_3 (10 mL), and the $^{225/227}$Ac eluted with 10 M HNO_3 (25 mL). Finally, the column was eluted with 0.1 M HNO_3 (10 mL) to elute radio-Ln.

2.8. Density functional theory (DFT) studies

Calculations were performed with the *Gaussian 09* [18], Revision D.01 software package using the B3LYP [19] and M06 [20] functionals. Standard 6–31+G* and 6–311+G** basis sets were used for main group elements and hydrogen for geometry optimization. F-elements were modeled using large-core (LC) relativistic effective core potential (RECP) and the associated (7s6p5d)/[4s3p3d] (Ac) and (7s6p5d)/[5s4p3d] [21] (Eu/Lu) basis sets. Additional 2f basis functions were added to the basis set of Ac and Ln when used in conjunction with 6–311+G** basis for light elements. Since LC RECP calculations include the 4f electrons in the core, they were performed on a pseudo singlet state configuration.

Frequency calculations at the B3LYP/LC/6–31+G* level were performed to ensure real vibrational modes for the minimum ground state structures and to provide zero point energies (ZPE). ZPE and thermal corrections (T = 298.15 K) were added to the total energy to obtain the Gibbs free energy. Thermal contributions to the gas phase Gibbs energies were calculated using standard molecular thermodynamic approximations [22], except that vibrational frequencies lower than 60 cm^{-1} were raised to 60 cm^{-1}. This procedure is based on a quasiharmonic approximation, which was first introduced by Truhlar et al. [23] and serves as a way to correct for the breakdown of the harmonic oscillator model for the free energies of low-frequency vibrational modes. Free energies of solvation were calculated at the B3LYP/LC/6–31+G* level using the IEF-PCM (IEF) [24] implicit solvation model with default settings.

3. Results and discussion

3.1. K_d studies

As mentioned above, some literature data exists for TODGA Ln K_d values –as determined via ICP-MS- for both HNO_3 and HCl media [9–16]. While the K_d values for Ce and La seem to be conclusive [16], the data appears largely inconclusive for the medium-heavy Ln in HCl media, especially at acid concentrations > 4 M.

3.1.1. Actinium-225 in HNO_3

Since available literature data [16] indicate strong retention (K_d >

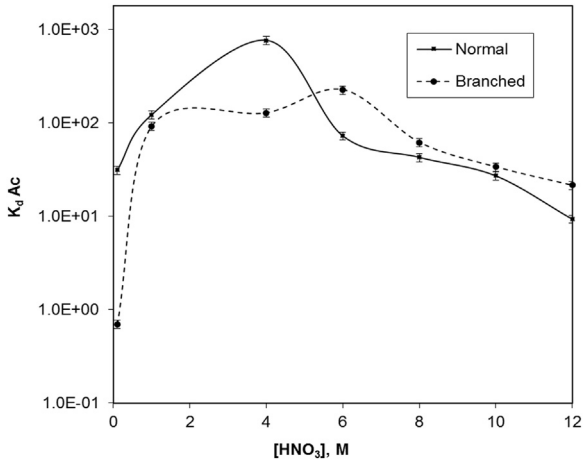

Fig. 1. Acid dependency of K_d for ^{225}Ac on normal (TODGA) and branched (TEHDGA) resins in HNO_3 (n = 3). Trend lines supplied.

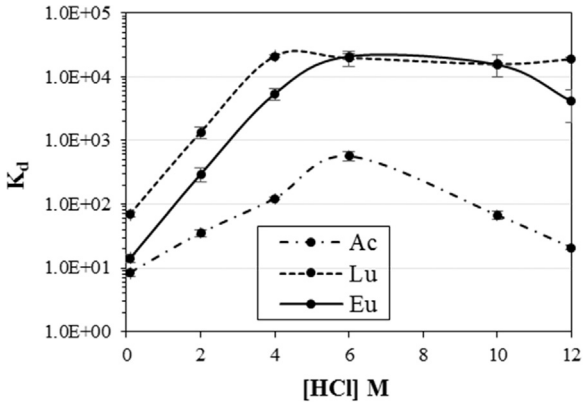

Fig. 2. Acid dependency of K_d for ^{225}Ac, ^{173}Lu, and ^{155}Eu with TODGA resin in HCl (n = 3). Trend lines supplied.

1000 g/mL) for all Ln in HNO_3 media at concentrations > 0.5 M in DGA based systems, the acquisition of new experimental Ln data for HNO_3 media was not considered in this work. Actinium sorption kinetics for both TODGA and TEHDGA have been evaluated in the literature [12]. For an exemplary HNO_3 concentration of 0.5 M, the study reported that batch sorption equilibria for both resins were reached after 120 ± 10 s, and equilibration times did not differ significantly for higher acid concentration. Fig. 1 shows Ac equilibrium distribution coefficients on TODGA and TEHDGA resins as a function of HNO_3 concentration as determined in this study. The data suggests that Ac K_d values in HNO_3 reach a maximum at 4 M (TODGA) and 6 M (TEHDGA) concentrations. Actinium sorption on TODGA is stronger than on TEHDGA (770 vs. 226 g/mL). These maximums are significantly lower than previously reported data for HNO_3 [12,15]. At lower and higher HNO_3 concentrations, we observed no significant difference between TODGA and TEHDGA, except for the lowest tested concentration (0.1 M HNO_3), where Ac shows less sorption on TEHDGA than on TODGA. In 10 M HNO_3 the K_d values for Ac decrease to roughly 50 allowing the separation of ^{225}Ac from Ln. It is important to note that no Ac K_d data have been published for HNO_3 concentrations beyond 6 M (TEHDGA) and 8 M (TODGA). But it is apparent from our data that only at about concentrations ≥ 10 M, HNO_3 begins to provide a high enough separation factor to separate ^{225}Ac from Ln efficiently. Results suggest that either TODGA or TEHDGA resin may be used to perform this separation.

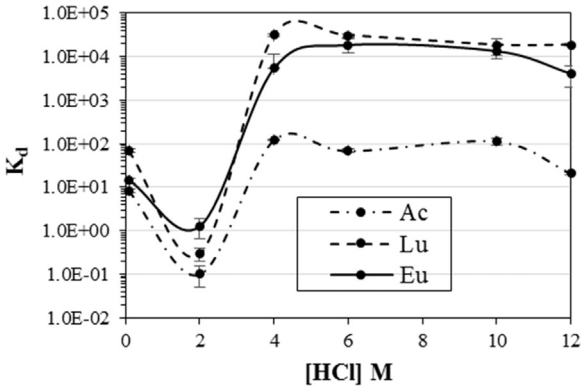

Fig. 3. Acid dependency of K_d for ^{225}Ac, ^{173}Lu, and ^{155}Eu with TEHDGA resin in HCl (n = 3). Trend lines supplied.

3.1.2. Actinium-225 and Ln in HCl

3.1.2.1. TODGA. Fig. 2 displays the equilibrium distribution coefficients for ^{225}Ac, ^{173}Lu, and ^{155}Eu with TODGA resin in HCl media. No Ac K_d literature data are available for HCl concentrations > 8 M. Published data for HCl ≤ 8 M [15] suggest a steady K_d increase for higher concentration, which, we found, is not the case; in fact, values decrease for higher concentrations, which can be exploited for fine purification from heavier Ln (Fig. 2). Data indicates that Ac exhibits the strongest sorption behavior at 6 M HCl, and Ac can be eluted with either 0.1 M or 10–12 M HCl. Lutetium attains a maximum K_d value of > 10,000 g/mL at HCl concentrations ≥ 4 M HCl; K_d decreases to < 100 g/mL in 0.1 M HCl. Europium reaches maximum K_d values of > 10,000 g/mL between 6 and 10 M HCl with an average K_d value of 18155 ± 2519 g/mL; K_d decreases steadily to < 300 g/mL at concentrations ≤ 2 M HCl.

3.1.2.2. TEHDGA. Fig. 3 shows the K_d values for ^{225}Ac, ^{173}Lu, and ^{155}Eu with TEHDGA resin tested in HCl media. Notably, the behavior of Ac with TEHDGA resin differs from the behavior with TODGA. With TEHDGA resin, Ac exhibits greatest affinity for the resin at 4–10 M HCl concentrations with an average K_d value of 102 ± 28 g/mL (compared to a maximum K_d of 568 ± 91 g/mL at 6 M HCl with TODGA). The weakest Ac adsorption is at 2 M HCl but, in contrast with TODGA resin, not with 0.1 or 12 M HCl. No Ac K_d literature data are available for HCl concentrations > 6 M. Published data [12] for HCl ≤ 6 M are generally lower than our results and again suggest a steady K_d increase for higher concentration, which, we found, is not the case; in fact, values remain constant for higher concentrations. Lutetium showed maximum sorption with concentrations ≥ 4 M HCl where the average K_d value plateaued at approximately 25,000 ± 7000 g/mL. Europium also exhibited this plateau behavior beyond 4 M HCl. Europium and lutetium, similar to actinium, showed weakest adsorption at 2 M HCl. K_d for Ac in HCl media differ significantly between TEHDGA and TODGA (Figs. 2 and 3). For TODGA, our study revealed that HCl concentrations > 4 M HCl are conducive to the separation of Ac from Ln. For the separation of Ln from each other, HCl media are required. Both resins in HCl concentrations of 0.1 M or 12 M HCl may be used.

3.2. Dynamic column separations in HNO_3 media

3.2.1. TODGA

The elution profile for $^{223/225}Ra$, ^{225}Ac, ^{173}Lu, and ^{155}Eu with TODGA resin in HNO_3 media is included in the Supporting information (Fig. S2). The first fraction (5 mL of 6 M HNO_3) contained more

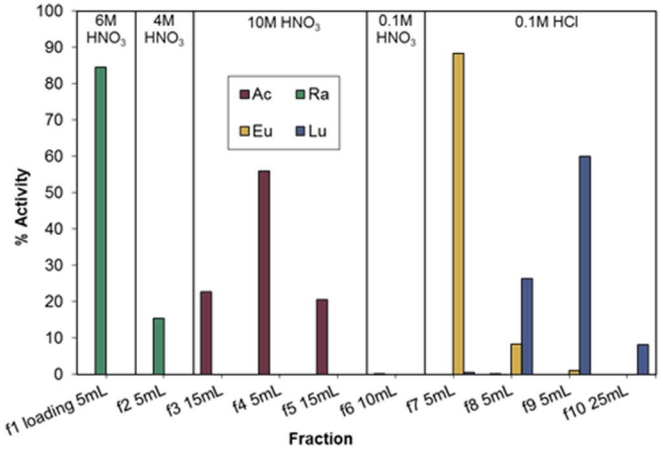

Fig. 4. Elution profile for $^{223/225}$Ra, ^{225}Ac, ^{173}Lu, and ^{155}Eu with TEHDGA resin in HNO_3 media and HCl for lanthanide elution.

than 84% of the Ra activity, and the remaining Ra (> 15%) was stripped with the 4 M HNO_3 wash (5 mL). With 10 M HNO_3 (35 mL total), more than 98% of the Ac activity was recovered. Lanthanides remained on the column and could be eluted using 0.1 M HCl.

3.2.2. TEHDGA

Fig. 4 shows the elution profile obtained for $^{223/225}$Ra, ^{225}Ac, ^{173}Lu, and ^{155}Eu for TEHDGA resin. The loading fraction (f1, 5 mL) contained > 89% of the initial Ra activity with no detectable amounts of other radionuclides. Washing with 4 M HNO_3 (f2, 5 mL) eluted the remaining Ra from the column prior to the Ac removal, which was achieved via elution with 35 mL (f3-f5) of 10 M HNO_3. Column contact with 0.1 M HNO_3 (f6, 10 mL) eluted 7% of the Eu activity and 1.5% of the Lu activity from the column. Subsequent contacts with 0.1 M HCl (f7-f10, 40 mL total volume) eluted > 90% and 92% of the Eu and Lu activities, respectively. Notably, fraction f7 contained 89% of the ^{150}Eu activity contaminated with only 0.4% of the original ^{173}Lu spike, while f9 + f10 contained 68% of all ^{173}Lu with ~ 1% of ^{150}Eu spike contamination, a significant Eu/Lu separation achieved with only 1 mL of resin bed. Actinium, Eu and Lu behavior in the dynamic column separation experiments in HNO_3 media are in good agreement with K_d results, demonstrating the possibility of separating Ac from Ln using either TEHDGA or TODGA. Radium elutes without sorption in 4–6 M HNO_3, and Ac is eluted with 10 M HNO_3. Lanthanides are retained on the column and can sequentially be eluted from the TEHDGA resin with 0.1 M HCl with a separation factor of ~ 5.

3.3. Irradiated target experiment and Ac separation in GBq quantities

The separation profile of Ac in 10 M HNO_3 on TEHDGA obtained utilizing Ac, Ra, Ba and Ln radioisotopes from a chemical separation run of an irradiated thorium target is included in the Supporting information (Fig S3). The 20 mL volume load solution contained most of the non-Ln (Ba, Ra, Ru) fission product activity. Additional washes with 4 M HNO_3 (2 × 5 mL) removed residual tracers of these radionuclides to a non-detectable level (thus achieving a separation factor ~ 10^4). More than 99% of the Ac eluted with the subsequent contact with 10 M HNO_3 (50 mL total), and Ln isotopes ^{140}La and ^{141}Ce eluted with the 0.1 M HCl contact (5 mL). As a considerable number of BV's of 10 M HNO_3 are required to elute the actinium from TEHDGA the elution profile of Ac was determined using remnants of a Ac/Ln separation campaign and is included in the Supporting information. The elution profile reveals that > 90% of the Ac can be recovered from the resin in 30 BV's of acid, but up to 50 BV's are required to recover the remainder of ^{225}Ac. This elution profile guided the procedure for recovery of Ac from a full scale target, and the separation method using TEHDGA has been integrated with the routine separation process for isolation of Ac from irradiated thorium targets. Further details associated with this separation will be covered in a forthcoming manuscript.

3.4. DFT studies

In order to better understand the DGA based separation of ^{225}Ac, ^{155}Eu and ^{173}Lu as observed in the dynamic column experiments at high concentrations of HNO_3, DFT modeling was carried out assuming a model ligand, N,N,N′,N′-tetramethyl-diglycolamide (TMDGA), which is a short aliphatic chain analog of TODGA and TEHDGA resin ligands (Fig. 5a) used in our experiments. This shortening of the ligand enables us to significantly save the computational resources, because finding the most stable configuration of the complexes containing TODGA or TEHDGA would be computationally prohibitively expensive. In addition, recent theoretical study shows that the chain length of hydrocarbon substituents has a little impact on the relative stability of actinide and lanthanide complexes [25]. Since the main focus of this work is on Ac/Ln separations, which are associated with a higher separation factors in HNO_3 media, calculations were performed under the assumption of nitrate ions as ligands. Based on solvent extraction and extraction chromatography data for extraction of Ln from nitrate media [13,26] and X-ray adsorption spectroscopy (XAS) studies [27], we presumed that homoleptic 1:3 complexes of $Ac^{III}/Eu^{III}/Lu^{III}$ with

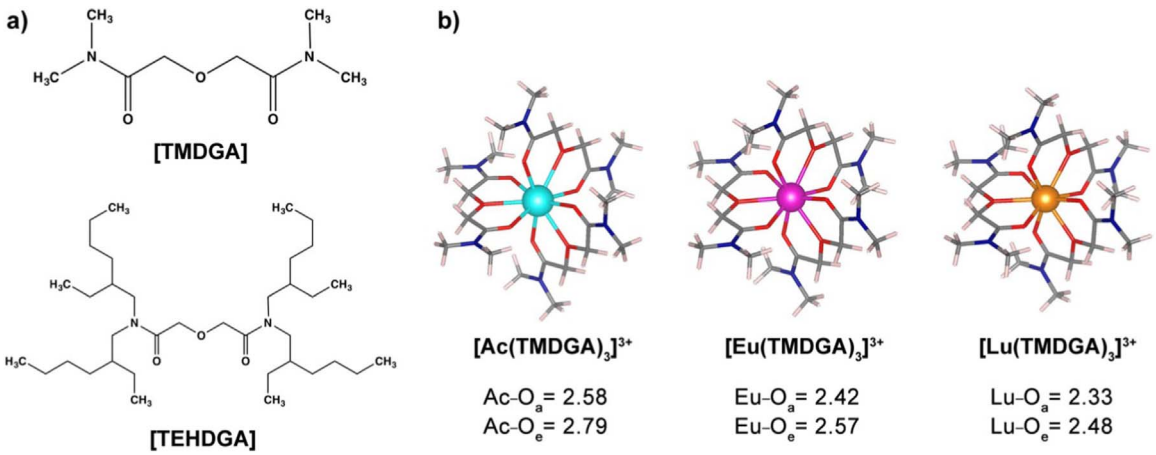

Fig. 5. a) Structures of the TMDGA and TEHDGA ligands; **b)** structures of the $[Ac(TMDGA)_3]^{3+}$, $[Eu(TMDGA)_3]^{3+}$, and $[Lu(TMDGA)_3]^{3+}$ complexes optimized with the M06/LC/6–311+G** method. Modeled M-O (M = Ac^{III}, Eu^{III}, and Lu^{III}) distances with amide (O_a) and ether (O_e) oxygen donor atoms are given in Å. Color scheme: Ac, turquoise; Eu, purple; Lu, orange; O, red; N, blue; C, grey; H, white. (For interpretation of the references to color in this figure legend, the reader is referred to the web version of this article.)

TODGA/TEHDGA prevailed in the studied systems at 4 M HNO_3, and thus the calculations were performed for the cationic $[M(TMDGA)_3]^{3+}$ (M = Ac^{III}, Eu^{III}, and Lu^{III}) complexes. The structures of the complexes optimized at the M06/LC/6–311+G** level of theory along with the average M-O interatomic distances between the donor oxygen atoms of TMDGA and the metal ions are shown in Fig. 5b.

There are nine donor oxygen atoms in the first coordination sphere of the metal ion. Since the obtained geometries of the complexes were found to be symmetric (close to D_3 point group symmetry), only two types of M–O bonds were reported: M-O_a (amide oxygen donor atoms) and M-O_e (ether oxygen donor atoms). The DFT calculated Eu-O_a and Eu-O_e bond lengths of 2.42 Å and 2.57 Å, respectively, for $[Eu(TMDGA)_3]^{3+}$ are in good agreement with the EXAFS-determined average Eu-O_a (2.40 Å) and Eu-O_e (2.50 Å) distances in the $[Eu(TODGA)_3]^{3+}$ complex [27]. Furthermore, the Eu-O_a and Eu-O_e bond parameters of the $[Eu(TMDGA)_3]^{3+}$ optimized structure (Fig. 5b) correspond well to those of the crystal structure of the Eu^{3+} complex (Eu-O_a = 2.40 Å, Eu-O_e = 2.49 Å) with a homologous ligand, N,N,N′,N′-tetraethyl-diglycolamide (TEDGA) [28]. Additionally, previous computational studies on $[Eu(TMDGA)_3]^{3+}$ reported the bond distances of 2.42 Å (Eu-O_a) and 2.62 Å (Eu-O_e) [29,30]. As seen from Fig. 5b, the corresponding Lu-O_a (2.33 Å) and Lu-O_e (2.48 Å) bond lengths in the $[Lu(TMDGA)_3]^{3+}$ complex were found to be 0.11 Å and 0.09 Å shorter than those of $[Eu(TMDGA)_3]^{3+}$, which is in agreement with the $[Lu(TEDGA)_3]^{3+}$ crystal structure data (Lu-O_a = 2.31 Å, Lu-O_e = 2.43 Å) [31]. To the best of our knowledge there are no reports on the EXAFS or crystallographic data for the $[Ac(TODGA)_3]^{3+}$ or $[Ac(TEDGA)_3]^{3+}$ complexes.

It is worth noting, however, that the calculated M-O_a and M-O_e distances decrease from 2.58 Å and 2.79 Å for $[Ac(TMDGA)_3]^{3+}$ to 2.42 Å and 2.57 Å for $[Eu(TMDGA)_3]^{3+}$ and to 2.33 Å and 2.48 Å for $[Lu(TMDGA)_3]^{3+}$ which is consistent with the contraction of ionic radii from 1.13 Å (Ac^{III}) to 0.95 Å (Eu^{III}) to 0.86 Å (Lu^{III}) [32]. The largest M–O bond lengths manifested in the $[Ac(TMDGA)_3]^{3+}$ complex (Fig. 5b) suggest that Ac^{III} would form the weakest bonds with oxygen donor atoms of TODGA. However, the analysis of bond distances alone is insufficient for predicting ligand selectivity across the Ln(III) series and for Ac(III) or other trivalent actinides, which requires careful thermodynamic consideration. Likewise, the application of simple geometric arguments [33] to rationalize higher ligand selectivity for larger metal ions forming five-membered chelate rings and for smaller metal ions forming six-membered chelate rings can be misleading and for TODGA leads to the wrong conclusions.

In addition, recent DFT investigations [30] of Am^{III}/Eu^{III} complexes with TEHDGA ligand suggest that chemical bonding analysis based on natural atomic orbitals and on the topology of electron density can estimate only the degree of covalency of Am^{III}/Eu^{III}-DGA bonds, but fails to predict better extraction of Eu^{III} than Am^{III} from the aqueous to the DGA organic phase observed in solvent extraction experiments [34].

In order to assess the separation efficiency of TMDGA for Ac^{III}, Eu^{III}, and Lu^{III}, we employed our recently developed computational approach to reproduce experimental aqueous selectivity for the size-based separation of trivalent actinides and Ln [35]. A competitive complexation of Ac^{III}, Eu^{III}, and Lu^{III} ions with TMDGA was modeled according to reactions (1) and (2):

$$Ac(TMDGA)_3^{3+}{}_{(aq)} + Eu(NO_3)_3(H_2O)_{3(aq)} \rightleftharpoons Ac(NO_3)_3(H_2O)_{3(aq)} + Eu(TMDGA)_3^{3+}{}_{(aq)},\ \mathbf{\Delta G_{aq}(Ac^{III}/Eu^{III})} \quad (1)$$

$$Ac(TMDGA)_3^{3+}{}_{(aq)} + Lu(NO_3)_3(H_2O)_{3(aq)} \rightleftharpoons Ac(NO_3)_3(H_2O)_{3(aq)} + Lu(TMDGA)_3^{3+}{}_{(aq)},\ \mathbf{\Delta G_{aq}(Ac^{III}/Lu^{III})} \quad (2)$$

The results of the free energy (ΔG_{aq}) calculations at different levels of theory (Table 2) confirm significantly higher selectivity of TMDGA for Ln^{III} over Ac^{III} in the presence of nitrate ions. This is in line with our experimental TODGA and TEHDGA resin results, showing that Ac^{III} can be selectively eluted at 10 M HNO_3, while Eu^{III} and Lu^{III} are retained on the resin. Overall, TODGA is expected to show a monotonic, but a nonlinear increase in selectivity with decreasing size of the metal ion, with a much larger slope for Ac^{III} and early Ln^{III}. These theoretical predictions are in excellent agreement with experimental data for Ln^{III}, in which the TODGA-type ligands demonstrate higher extraction efficiency for the smaller (heavier) Ln [16,36] and stronger retention in the aqueous phase in the presence of TEDGA as an aqueous hold back reagent [34].

Table 2
Calculated Gibbs free energies for eqs. **(I)** and **(II)**.

Method	ΔG_{aq} (Ac^{III}/Eu^{III}) [kJ/mol (kcal/mol)]	ΔG_{aq} (Ac^{III}/Lu^{III}) [kJ/mol (kcal/mol)]
B3LYP/LC/6–311+G**//IEF	– 54.52 (– 13.03)	– 68.70 (– 16.42)
B3LYP/LC/6–31+G*//IEF	– 47.28 (– 11.30)	– 60.50 (– 14.46)
M06/LC/6–311+G**//IEF	– 55.35 (– 13.23)	– 69.37 (– 16.58)
M06/LC/6–31+G*//IEF	– 48.99 (– 11.71)	– 62.26 (– 14.88)

4. Conclusion

We provided radioanalytical proof that diglycolamide based resins TODGA and TEHDGA are suitable for high-yield, high-purity separation of Ac isotopes from Ra and fission product lanthanides in the context of ^{225}Ac production via proton induced nuclear reaction on thorium (^{232}Th) targets. Especially in the higher HNO_3 and HCl concentration range, Ac and Ln sorption behavior on DGA has not been conclusively described in the literature so far. Hence, we measured equilibrium distribution coefficients for the sorption of Ac^{3+}, Eu^{3+} and Lu^{3+} cations on both resin types in HCl media and in HNO_3 for Ac^{3+} over a wide concentration range for the first time. Previous measurements were only partially confirmed by our results. For Ac in particular, measured affinity in HNO_3 was lower than reported previously. On the other hand, slightly higher affinity in HCl media was observed. Lower affinity in HNO_3 corroborates the assumption that both resins TEHDGA and TODGA can be used in HNO_3 to separate Ac from Ln; TEHDGA can in principle be used to separate Ln from each other.

Experimentally, we observed that Ac and the 4f- elements exhibited largely different DGA sorption behavior. This initially unexpected behavior, however, can be plausibly explained on the ground of density functional theory (DFT) modeling. For this purpose, the structures of Ac^{III}, Eu^{III}, and Lu^{III} nitrate complexes with a model ligand (TMDGA) were investigated using large-core (LC) relativistic effective core potential (RECP) and associated (7s6p5d)/[4s3p3d] (Ac) and (7s6p5d)/[5s4p3d] (Eu/Lu) basis sets. The largest bond distances between Ac^{III} and the ligand donor atoms observed in the $[Ac(TMDGA)_3]^{3+}$ complex suggest weaker interactions between Ac^{III} and TMDGA compared to those of Eu^{III}-TMDGA and Lu^{III}-TMDGA. According to the thermodynamic analysis, calculated Gibbs energies $\Delta G_{aq}(Ac^{III}/Eu^{III})$ and $\Delta G_{aq}(Ac^{III}/Lu^{III})$ of the competitive complexation reactions are negative, denoting much higher selectivity of TMDGA for Eu^{III} and Lu^{III} over Ac^{III} in the presence of nitrate ions, which is in agreement with experimental data. DFT results thus provide the essential foundation explaining the energetic differences underpinning Ac-Ln discrimination with DGA resins. Although Ln elements are often used as stable Ac surrogates, results show that Ac chemistry cannot be simply predicted from Ln behavior under comparable circumstances.

Acknowledgement

This material is based upon work supported by the United States Department of Energy, Office of Science, Office of Nuclear Physics, via

an award from the Isotope Development and Production for Research and Applications subprogram under contract number DE-AC52-06NA253996. We also thank the technical assistance provided by LANL C-IIAC and LANSCE-AOT groups. The computational part of this work was supported by the Fuel Cycle Research and Development Program, Office of Nuclear Energy, U.S. Department of Energy and used resources of the National Energy Research Scientific Computing Center, a US DOE Office of Science supported user facility.

Appendix A. Supplementary material

Supplementary data associated with this article can be found in the online version at doi:10.1016/j.talanta.2017.07.057.

References

[1] M.W. Brechbiel, Dalton Trans. 43 (2007) 4918–4928.
[2] E. Dadachova, Semin. Nucl. Med. 40 (2010) 204–208.
[3] M. Miederer, D.A. Scheinberg, M.R. McDevitt, Drug Deliv. Rev. 60 (2008) 1371–1382.
[4] (a) C. Kratochwil, F.L. Giesel, F. Bruchertseifer, W. Mier, C. Apostolidis, R. Boll, K. Murphy, U. Haberkorn, A. Morgenstern, Eur. J. Nucl. Med. Mol. Imaging 41 (2014) 2106–2119;

(b) C. Kratochwil, F. Bruchertseifer, F.L. Giesel, M. Weis, F.A. Verburg, F. Mottaghy, K. Kopka, C. Apostolidis, U. Haberkorn, A. Morgenstern, J. Nucl. Med. 57 (2) (2016) 1941–1944.
[5] IAEA, Alpha emitting radionuclides and radiopharma-ceuticals for therapy, Technical Meeting, Vienna, 2013.
[6] J.W. Weidner, S.G. Mashnik, K.D. John, F. Hemez, B. Ballard, H. Bach, E.R. Birnbaum, L.J. Bitteker, A. Couture, D. Dry, M.E. Fassbender, M.S. Gulley, K.R. Jackman, J.L. Ullmann, L.E. Wolfsberg, F.M. Nortier, Appl. Radiat. Isot. 70 (11) (2012) 2602–2607.
[7] R.A. Boll, D. Malkemus, S. Mirzadeh, Appl. Radiat. Isot. 62 (5) (2005) 667–679.
[8] V. Radchenko, J.W. Engle, J.J. Wilson, J.R. Maassen, F.M. Nortier, W.A. Taylor, E.R. Birnbaum, L.A. Hudston, K.D. John, M.E. Fassbender, J. Chromatogr. A 1380 (2015) 55–63.
[9] K. Van Hecke, G. Modolo, J. Radioanal. Nucl. Chem. 261 (2) (2004) 269–275.
[10] E.P. Horwitz, D.R. McAlister, A.H. Bond, R.E. Barrans Jr, Solv. Extr. Ion Exch. 23 (2005) 319–344.
[11] S.A. Ansari, P.N. Pathak, M. Husain, A.K. Prasad, V.S. Parmar, V.K. Manchanda, Talanta 68 (2006) 1273–1280.
[12] B. Zielinska, C. Apostolidis, F. Bruchertseifer, A. Morgenstern, Solv. Extr. Ion Exch. 25 (2007) 339–349.
[13] E.P. Horwitz, D.R. McAlister, A.H. Bond, R.E. Barrans Jr, Solvent Extr. Ion Exch. 26 (2008) 12–24.
[14] M. Husaina, S.A. Ansaric, P.K. Mohapatrac, R.K. Guptab, V.S. Parmara, V.K. Manchandac, Desalination 229 (2008) 294–301.
[15] S.L. Maxwell, B.K. Culligan, R.C. Utsey, D.R. McAlister, E.P. Horwitz, J. Radioanal. Nucl. Chem. 295 (2013) 2181–2188.
[16] A. Pourmand, N. Dauphas, Talanta 81 (2010) 741–753.
[17] J.R. Griswold, D.G. Medvedev, J.W. Engle, R. Copping, J.M. Fitzsimmons, V. Radchenko, J.C. Cooley, M.E. Fassbender, D.L. Denton, K.E. Murphy, A.C. Owens, E.R. Birnbaum, K.D. John, F.M. Nortier, D.W. Stracener, L.H. Heilbronn, L.F. Mausner, S. Mirzadeh, Appl. Radiat. Isot. 118 (2016) 366–374.
[18] M.J. Frisch, Gaussian 09, Revision D.01, Gaussian, Inc., Wallingford, CT, 2009.
[19] (a) A.D. Becke, J. Chem. Phys. 98 (1993) 5648–5652;

(b) C. Lee, W. Yang, R.G. Parr, Phys. Rev. B 37 (1988) 785–789.
[20] Y. Zhao, D.G. Truhlar, Theor. Chem. Acc. 120 (2008) 215–241.
[21] M. Dolg, H. Stoll, A. Savin, H. Preuss, Theor. Chem. Acc. 75 (1989) 173–194.
[22] D.A. McQuarrie, J.D. Simon, Molecular Thermodynamics, University Science Books, USA, 1999.
[23] R.F. Ribeiro, A.V. Marenich, C.J. Cramer, D.G. Truhlar, J. Phys. Chem. 115 (2011) 14556–14562.
[24] J. Tomasi, B. Mennucci, R. Cammi, Chem. Rev. 105 (2005) 2999–3094.
[25] J.H. Lan, W.Q. Shi, L.Y. Yuan, Y.L. Zhao, J. Li, Z.F. Chai, Inorg. Chem. 50 (2011) 9230–9237.
[26] (a) M.P. Jensen, in: Proceedings of the 18th International Solvent Extraction Conference, Tucson, AZ, United States, Sept. 15–19, 2008, ed. B. A. Moyer, Canadian Institute of Mining, Metallurgy and Petroleum, Montreal, Canada, 2008, vol. II, pp. 1029. (b) T. Yaita, A. W. Herlinger , P. Thiyagarajan, M. P. Jensen, Solvent Extr. Ion Exch., 22, 2004, 553–571. (c) Y. Sasaki , P. Rapold, M. Arisaka, M. Hirata, T. Kimura , C. Hill, G. Cote, Solvent Extr. Ion Exch., 25,2007, 187–204.
[27] M.R. Antonio, D.R. McAlister, E.P. Horwitz, Dalton Trans. 44 515-521; (b) A. Wilden, in: Proceedings of the First SACSESS International Workshop, Warsaw, Poland, 22–24 April, ⟨http://www.sacsess.eu/Docs/IWSProgrammes/15-SACSESSIWS-Wilden.pdf⟩.
[28] T. Kawasaki, S. Okumura, Y. Sasaki, Y. Ikeda, Bull. Chem. Soc. Jpn. 87 (2014) 294–300.
[29] M. Kaneko, M. Watanabe, T. Matsumura, Dalton Trans. 45 (2016) 17530–17537.
[30] J. Narbutt, A. Wodyński, M. Pecul, Dalton Trans. 44 (2015) 2657–2666.
[31] S. Okumura, T. Kawasaki, Y. Sasaki, Y. Ikeda, Bull. Chem. Soc. Jpn. 87 (2014) 1133–1139.
[32] R.D. Shannon, C.T. Prewitt, Acta Cryst. Sect. A B25 (1969) 925–946.
[33] R.D. Hancock, A.E. Martell, Chem. Rev. 89 (1989) 1875–1914.
[34] (a) Y. Sasaki, Y. Kitatsuji, Y. Tsubata, Y. Sugo, Y. Morita, Solvent Extr. Res. Dev. Jpn. 18 (2011) 93–101;

(b) A.V. Gelis, G.J. Lumetta, Ind. Eng. Chem. Res. 53 (2014) 1624–1631.
[35] A.S. Ivanov, V.S. Bryantsev, Eur. J. Inorg. Chem. 21 (2016) 3474–3479.
[36] R.J. Ellis, D.M. Brigham, L. Delmau, A.S. Ivanov, N.J. Williams, M.N. Vo, B. Reinhart, B.A. Moyer, V.S. Bryantsev, Inorg. Chem. 56 (3) (2017) 1152–1160.